Innate immune evasion mechanisms utilized by Ectromelia virus
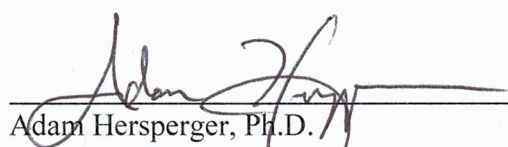
Tiffany Frey

Candidate for the degree

Bachelor of Sciences

Submitted in partial fulfilment of the requirements for

College Honors

Departmental Distinction in Biology

_____
Adam Hersperger, Ph.D.

_____
Stephen Mech, Ph.D.

_____
Ian Rhile, Ph.D.

F. Wilbur Gingrich Library
Special Collections Department
Albright College

Release of Senior Thesis

I hereby deliver, give, and transfer property, rights, interest in and legal rights thereto which I had, have, or may have concerning the Senior Honors Thesis described below to the Special Collections Department of the F. Wilbur Gingrich Library at Albright College as an unrestricted gift. While copyright privileges will remain with me, the author, all privileges to reproduce, disseminate, or otherwise preserve the Senior Honors Thesis are given to the Special Collections Department of the Gingrich Library. I place no restrictions on this gift and hereby indicate this by signing below.

Title: Innate immune evasion mechanisms utilized by Ectromelia virus

Signature of Author: _Tiffany Frey_ Date: 4/17/2017

Printed Name of Author: _Tiffany Frey_

Street Address: _745 Pennsylvania Avenue_

City, State, Zip Code: _Bangor, PA 18013_

Abstract

Most orthopoxviruses, including vaccinia virus (VACV), contain genes in the E3L and K3L families. The protein products of these genes (termed E3 and K3, respectively) have been previously shown to combat protein kinase R (PKR), a host defense pathway. Interestingly, ectromelia virus (ECTV) contains an E3L orthologue but does not possess an intact K3L gene. This study was performed to gain insight on how ECTV can still efficiently evade PKR despite lacking K3L. Relative to VACV, ECTV displayed less accumulation of dsRNA in several cell lines. Further, the ribonuclease L (RNase L) pathway was activated only in VACV-infected but not ECTV-infected cells, indicating the presence of less detectable dsRNA during the replication cycle of ECTV. Additionally, ECTV demonstrated a protracted replication cycle relative to VACV. Overall, it seems that ECTV produces less detectable dsRNA by slowing its replication cycle, allowing it to efficiently evade detection by PKR and RNase L while lacking K3L.

Introduction

Poxviruses are large, double-stranded DNA (dsDNA) viruses that replicate in the cytoplasm of cells (Chen et al. 2003). Ectromelia virus (ECTV), or mousepox, is a member of the *Poxviridae* family. Natural ECTV infection occurs in mice through abrasions in the skin, leading to subsequent dissemination to other organs (Fenner 1947). Disease manifestation then results in pockmark lesions, similar to those seen during the smallpox pandemic (Fenner 1947). Vaccinia virus (VACV) is another orthopoxvirus that is closely related to ECTV and was used as a vaccine to combat smallpox.

During infection with a dsDNA virus, the formation of double-stranded RNA (dsRNA) is commonly seen. This molecule is formed primarily because viral genomes are small and the genes tightly pack together, causing transcription machinery to often read through one gene into the next gene. Additionally, transcription often occurs in a convergent fashion in which RNA polymerase reads from both DNA strands simultaneously. The combination of read through and convergent transcription often results in pieces of RNA that are complimentary to each other. These RNA molecules can then base pair, causing the formation of dsRNA within host cells. This event has been shown to primarily occur during late transcription when intermediate and late genes are expressed (Jacobs and Langland 1996). The anti-poxvirus drug isatin beta-thiosemicarbazone (IBT), which was used in the present study, has been shown to artificially increase the amount of dsRNA formed within VACV-infected cells (Cresawn et al. 2007).

While dsRNA forms during the replication of poxviruses, this molecule is not produced in mammalian host cells, causing it to serve as a potent danger signal to the host immune system. Detection of dsRNA subsequently leads to the activation of innate immune pathways within the host cells, including protein kinase R (PKR) and ribonuclease L (RNase L). Both halt translation,

inhibiting viral replication. PKR phosphorylates the eukaryotic translation initiation factor, eIF2α, causing cap-dependent translation in the cell to be halted. RNase L is activated by the detection of large amounts of dsRNA and leads to the degradation of all RNA within the cell (Díaz-Guerra et al. 1997).

Because hosts have evolved mechanisms to detect and blunt viral replication, poxviruses have also evolved genes to evade the immune system and allow for replication. Two of these immune evasion genes are E3L and K3L. E3L codes for the E3 protein and is found in both ECTV and VACV. The protein product of E3L, E3, acts by directly binding to dsRNA, shielding it from detection by immune cells. This was initially discovered because of its ability to bind to Poly(I:C), a synthetic dsRNA mimic, from extracts of VACV-infected cells (Watson et al. 1991; Chang et al. 1992). E3 shielding of dsRNA prevents the activation of PKR and RNase L pathways. E3 has also demonstrated importance in the overall replication of ECTV and VACV, with viral strains lacking functional E3 unable to replicate in certain species (Beattie 1996).

The K3L gene codes for a protein product (termed K3) that serves as a mimic of eIF2α. Production of this protein allows the competition of binding to PKR between the cellular eIF2α and the mimic produced by K3L, thereby making PKR activation less likely to occur. While many poxviruses contain the K3L gene, ECTV does not encode a full-length version of K3 due to a premature stop codon, leading to a non-functional protein product (Chen et al. 2003; Smith and Alcami 2002).

This study aimed to gain insight on how ECTV can still efficiently evade PKR despite lacking K3L. The hypothesis that infection with ECTV would consistently lead to the detection of less free dsRNA relative to VACV was tested. Additionally, this study intended to address the potential mechanisms that lead to less detectable dsRNA formation in ECTV.

Methods

Cells and culture methods:

Wild-type BSC1 and RK13 (gift of Dr. Stefan Rothenburg) cell lines were used during this study. Two cell lines were also utilized that constitutively expressed the E3 protein of VACV: BSC1+E3L and RK13+E3L (both gift of Dr. Stefan Rothenburg). The RK13+E3L cells have been described in previously published reports (Rahman et al. 2013; Hand et al. 2015). These stably transfected cells were maintained in the continuous presence of 500 μg/mL Geneticin/G418 (Gemini BioProducts) to maintain high levels of E3, which were consistently ≥90% as determined by flow cytometry. All cell lines were cultured in Dulbecco's Modified Eagle Medium (DMEM; Invitrogen) supplemented with 5% fetal bovine serum (FBS; Gemini BioProducts), and penicillin-streptomycin (Gemini BioProducts). All cells were maintained at 37 °C in a 6% CO_2 incubator and split when they reached approximately 80% confluency. In some experiments, as indicated, cells were kept at 30 °C and 6% CO_2.

Viruses:

The following viruses were used during the course of this work: ECTV wild-type (Moscow strain; gift of Dr. Laurence Eisenlohr), ECTV expressing GFP [Moscow background; gift of Dr. Luis Sigal (Fang et al. 2008)] VACV wild-type (Western Reserve strain; gift of Dr. Laurence Eisenlohr), VACV expressing GFP (Western Reserve background; BEI resources NR-624), and VACVΔE3LΔK3L (Copenhagen background). VACVΔE3LΔK3L (gift of Dr. Stefan Rothenburg) was constructed using standard homologous recombination techniques. This mutant virus expresses green fluorescent protein (GFP); more detailed information concerning this virus

can be found in Brennan et al. (2014). In some experiments, cytosine β-D-arabinofuranoside (Ara-C; Sigma-Aldrich) was used at 50 μg/mL to block viral DNA replication and prevent late gene expression.

Microscopy:

Phase-contrast microscopy was performed using an Accu-Scope model 3032 with an attached Micrometrics camera. Fluorescent microscopy was carried out using a Zeiss Axiostar plus epifluorescent microscope and images were captured with an Optronics camera system. All images were prepared for publication using ImageJ software. Cells were grown in four-well chamber slides (Thermo Scientific Nunc Lab-Tek II), infected with either ECTV or VACV (MOI=10), and fixed at the indicated time points with 5% formalin for 10 min. at room temperature. For virus factory analysis, glass coverslips were then immediately mounted onto the slide with ProLong Gold antifade reagent with 4',6-diamidino-2-phenylindole (DAPI; Invitrogen) and allowed to cure overnight prior to visualization. For dsRNA staining, cells were fixed, permeabilized in acetone (Fisher Scientific) at -20° C for 10 min., incubated in blocking buffer [2% bovine serum albumin (BSA; Gemini BioProducts) and 2% FBS (Gemini BioProducts) in 1x PBS] for 45 min., and then incubated for 45 min. with anti-dsRNA monoclonal antibody (J2 antibody; Scicons). After washing with 1x PBS, Alexa Fluor 568 goat anti-Mouse IgG2a (Invitrogen) diluted in blocking buffer was applied for 35 min. Glass coverslips were then mounted as described above with ProLong Gold antifade reagent containing DAPI. Methods were also later used for dsRNA detection in cowpox virus (CPXV). For surface B5 staining, unpermeabilized cells were incubated - after fixation - in blocking buffer for 45 min. and then an anti-B5 monoclonal antibody (BEI resources NR-553; clone VMC-22) was added

for 45 min. After washing with 1x PBS, Alexa Fluor 568 goat anti-Mouse IgG1 (Invitrogen) diluted in blocking buffer was applied to cells for 35 min. Finally, glass coverslips were mounted, as above, with ProLong Gold antifade reagent with DAPI.

Transfection of RK13 plain or RK13+E3L cells with 1μg Poly(I:C) was also performed followed by dsRNA staining using the J2 antibody, as described above. Additionally, a quality control experiment was performed to rule out the possibility that there are differences in the ability to transfect each cell line. To determine this, both RK13 and RK13+E3L cells were transfected with 1 μg Poly(I:C) conjugated to FITC, which fluoresces green upon excitation.

Flow cytometry:

Flow cytometry data were collected using a FACSCalibur instrument (BD Biosciences) equipped with both a red and blue laser. A minimum of 50,000 total cells were collected for each sample. The acquired data were analyzed using FCS Express 4 Flow Cytometry (De Novo Software; version 4.07). To measure the levels of dsRNA, infected cells (MOI=10) were harvested via trypsin digestion and washed once with 1x PBS containing 1% BSA (Gemini BioProducts). Cells were then fixed and permeabilized for 20 min. using the Cytofix/Cytoperm kit (BD Biosciences) per the manufacturer's instructions. After the fixation and permeabilization step, cells were washed twice with 1x Perm/Wash Buffer (BD Biosciences) before addition of an anti-dsRNA monoclonal antibody (J2 antibody; Scicons) to the cells. After 45 min. of incubation at room temperature, the cells were washed once with 1x Perm/Wash Buffer followed by the addition of anti-mouse IgG2a APC (eBioscience) for an additional 45 min. A final wash with 1x Perm/Wash Buffer was then performed prior to the addition of ~0.5 mL of 2% paraformaldehyde (Electron Microscopy Sciences) to each tube.

Plaque reduction assay:

Plaque reduction assays were performed to determine the effect of isatin beta-thiosemicarbazone (IBT) on virus growth and subsequent plaque formation. Cells were seeded in six-well plates, allowed to incubate overnight, and were confluent the following day. The cells were then infected with approximately 75 plaque forming units of either ECTV or VACV in growth media containing a reduced FBS concentration (2% instead of 5%). After 1.5 hours to allow for virus adsorption and entry, the infection media was exchanged for standard growth media. IBT was then added to the cells at the following concentrations: 0, 1, 5, 10, 15, and 45 µM. It is known that VACV plaques can be visualized after two days of incubation (Earl and Moss 2001) while ECTV plaque visualization needs a minimum of four to five days of incubation (Hand et al. 2015). Therefore, plaques were visualized using crystal violet solution after two days of incubation for VACV and five days for ECTV.

RNase L activity assay:

BSC1 or BSC1+E3L cells were plated in six-well culture plates one day prior and in sufficient numbers to be 80-90% confluent at the time of infection. Cells were either mock infected or infected (MOI=10) with the indicated viruses. Total RNA was isolated at the indicated times post-infection using the PureLink RNA Mini kit (Invitrogen) following the manufacturer's instructions. RNA electrophoresis was performed using a "bleach gel" (Aranda et al. 2012), which contained 1% agarose and 1% bleach (Clorox; 6% sodium hypochlorite) in a TBE buffer-based gel. Each lane contained 5 mg of RNA. For visualization of rRNA bands, the gel was stained with ethidium bromide.

Results

ECTV forms less free dsRNA than VACV:

Fluorescent microscopy utilizing the J2 antibody, which specifically recognizes dsRNA but not single-stranded RNA or DNA (Weber et al. 2006), revealed higher levels of detectable dsRNA in VACV-infected cells than in ECTV-infected cells (Fig. 1A). Treatment of infected cells with Ara-C, which inhibits DNA replication and subsequent intermediate and late gene activity, prevented dsRNA detection in VACV-infected cells (Fig. 1B). This suggests that most of the dsRNA signal detected was a result of intermediate and/or late gene transcription. A flow cytometric assay utilizing the same anti-dsRNA J2 antibody confirmed that more free dsRNA was being produced during VACV infection than ECTV infection. These results also demonstrate that more free dsRNA is produced in BSC1 cells infected with VACV than ECTV (Fig. 1C and 1D). Fluorescent microscopy in CPXV-infected BSC1 cells showed virus factory formation similar to that of VACV (Fig. 1E). Additionally, dsRNA formation was comparable to VACV (Fig. 1F).

E3 masks the detection of dsRNA by J2:

Transfection of RK13 plain or RK13+E3L cells with Poly(I:C) showed that RK13+E3L cells display less dsRNA positivity in comparison to RK13 plain cells (Fig. 2A). The quality control experiment performed to rule out the possibility that the RK13+E3L cells were less able to be transfected than RK13 plain cells showed equal amounts of fluorescence between the two cell types, indicating that the transfection efficiency between cell lines was comparable (Fig. 2A). Flow cytometric methods to analyze dsRNA positivity in BSC1 and BSC1 cells expressing

the E3 protein (BSC1+E3L) revealed that BSC1+E3L cells had a lower dsRNA signal compared to BSC1 plain cells (Fig. 2B).

The infection time course with VACVΔE3LΔK3L in BSC1 cells shows that approximately 50% of cells positive for detectable dsRNA four hrs. post-infection, followed by an increase to approximately 85% at the subsequent time points (Fig. 2C). In contrast, wild-type VACV did not show significant free dsRNA formation until after 12 hrs. post-infection (Fig. 2C). Flow cytometric data between VACV, VACVΔE3LΔK3L, and ECTV demonstrate that VACVΔE3LΔK3L-infected cells show a lower fluorescence intensity for dsRNA formation (Fig. 2D).

RNase L activation is only seen in VACV after 12 hrs. post infection:

RNase L activation assays showed that ECTV did not induce the activation of RNase L at either time point (8 or 18hrs.), while VACV showed RNase L activation at 18 hours, but not 8 hours (Fig. 3A). RNase L activation assays in BSC1+E3L cells at 18 hrs. post-infection found that RNase L was not activated (Fig. 3A). Additionally, AraC was utilized with VACV-infected cells, which also reversed RNase L activation (Fig. 3B). Upon assays in VACVΔE3LΔK3L, RNase L was activated much earlier (Fig. 3C).

ECTV and VACV both display sensitivity to IBT:

Previous studies demonstrate that treatment of VACV-infected cells with IBT leads to elongated viral transcripts during intermediate and late time points, causing higher amounts of dsRNA formation (Prins et al. 2004; Bayliss and Condit 1993). Based on this, it was predicted that IBT treatment would lead to higher dsRNA levels. A significant increase in the frequency of dsRNA-positive cells following infection with VACV and treatment with 45 μM IBT was

observed (Fig. 4A and 4B). Interestingly, there was also a dramatic increase in dsRNA staining for ECTV-infected cells that had been IBT treated (Fig. 4A and 4B). Because increased dsRNA formation was seen in VACV-infected cells, the state of RNase L activation at 18 hrs. was tested and showed further RNA degradation in VACV-infected cells that had the addition of IBT relative to VACV only (Fig. 4C). Plaque reduction assays using BSC1 cells did not reveal a significant difference in IBT sensitivity between the two viruses (Fig. 4D). ECTV was statistically more resistant at low concentrations of the drug but was fully inhibited – similar to VACV – at 45 µM IBT (Fig. 4D).

ECTV shows protracted replication kinetics compared to VACV:

The plaque formation time course using phase contrast microscopy with ECTV and VACV engineered to express GFP showed that VACV forms sizable plaques by day 2, while ECTV did not show similar plaque formation until day 5 (Fig. 6A). Further, virus factory formation demonstrated that VACV takes 4 hours to form virus factories in 80% of cells, while the equivalent is not seen in ECTV until approximately 12 hrs. post-infection (Fig, 6A). Additionally, the percent of cells positive for GFP overtime and the median fluorescence intensity between ECTV and VACV-infected cells showed that GFP percent positivity and median fluorescent intensities were higher in VACV than ECTV, with ECTV showing approximately a 4 hr. delay relative to VACV (Fig. 6C and 6D).

<u>*VACV infection performed at 30 °C shows slower replication kinetics and reduced dsRNA*</u>

<u>*formation:*</u>

Replication kinetics were analyzed by comparing VACV infections at 37 °C, the standard temperature, with VACV infections at 30 °C in BSC1 cells. Staining and analysis of virus factory presence and size indicated that VACV grown at 30 °C had a delay relative to VACV at 37 °C in both factors (Fig. 7A, 7B, 7C). Cell surface expression of the viral B5 protein, which is a late (i.e. post-DNA replication) infection event, was also analyzed. Consistent with the virus factory data, there was a marked delay in the appearance and relative abundance of cell surface B5 when VACV was grown at 30 °C (Fig. 7D). Fluorescent microscopy staining for the presence of dsRNA to determine if replication kinetics would alter the amount of detectable dsRNA revealed that VACV-infected cells incubated at 30 °C produced much less dsRNA than VACV-infected cells incubated at 37 °C (Fig. 7E).
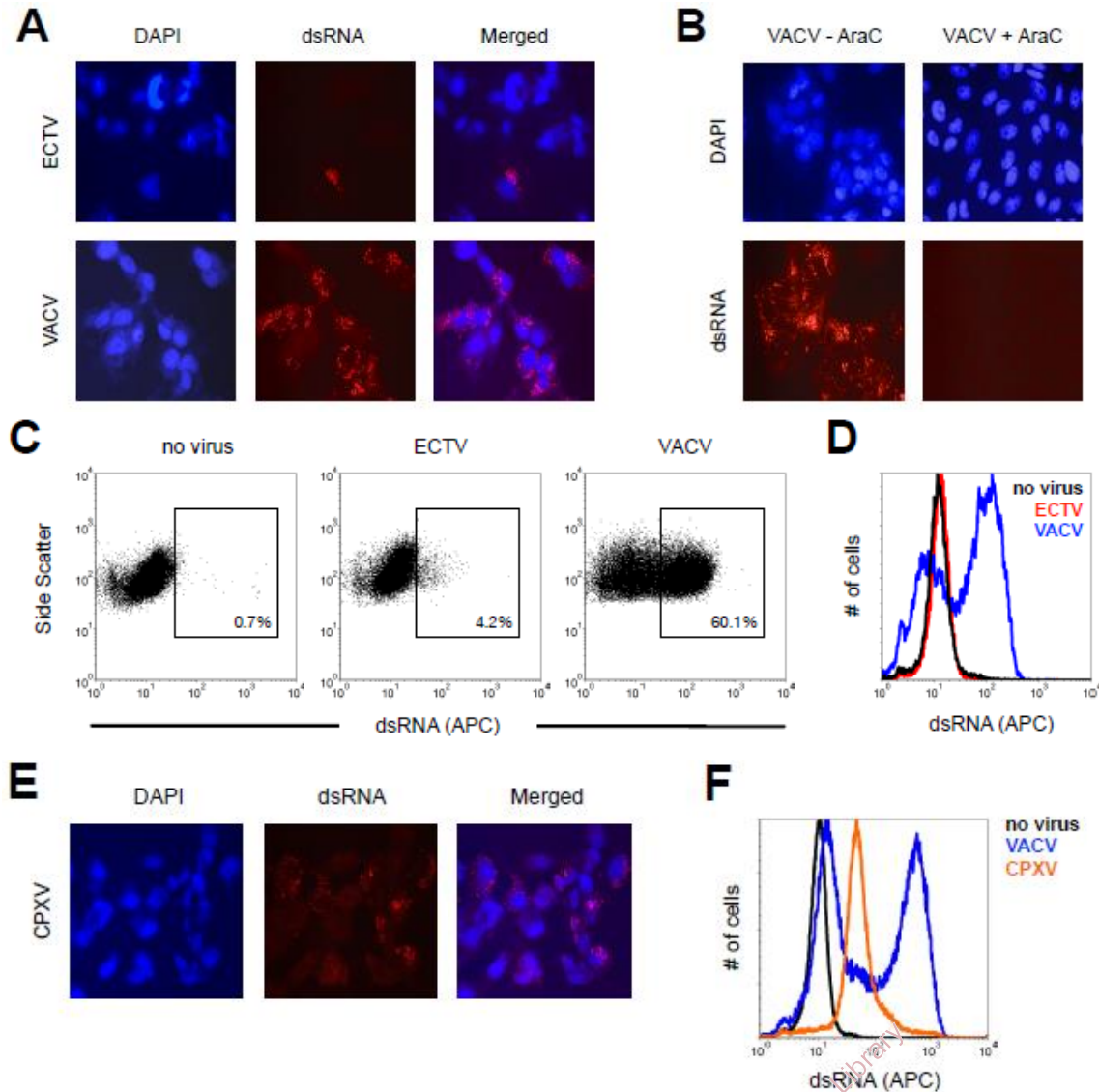
Albright College Gingrich Library

Figure 1: The accumulation of dsRNA varies greatly after infection with ECTV and VACV. (A) BSC1 cells were infected (MOI=10) with either ECTV or VACV for 24 hrs. prior to antibody staining for cell nuclei/virus factories and dsRNA. Images are representative of three independent trials. **(B)** BSC1 cells were infected (MOI=10) with VACV for 24 hrs. prior to staining for cell nuclei/virus factories and dsRNA. Ara-C was added at the time of infection. Images are representative of three independent trials. **(C)** BSC1 cells were infected (MOI=10) with either ECTV or VACV for 24 hrs. prior to staining for dsRNA using a secondary antibody conjugated to APC. Positive gates were drawn based upon the uninfected condition. Data are representative of three independent trials. **(D)** Flow cytometric data shown in the previous figure panel is depicted in histogram format. **(E)** BSC1 cells were infected (MOI=10) with CPXV for 24 hrs. prior to staining for dsRNA using methods described in (A). **(F)** Flow cytometric data comparing CPXV and VACV staining for dsRNA using a secondary antibody conjugated to APC. Positive gates were drawn based upon the uninfected condition.
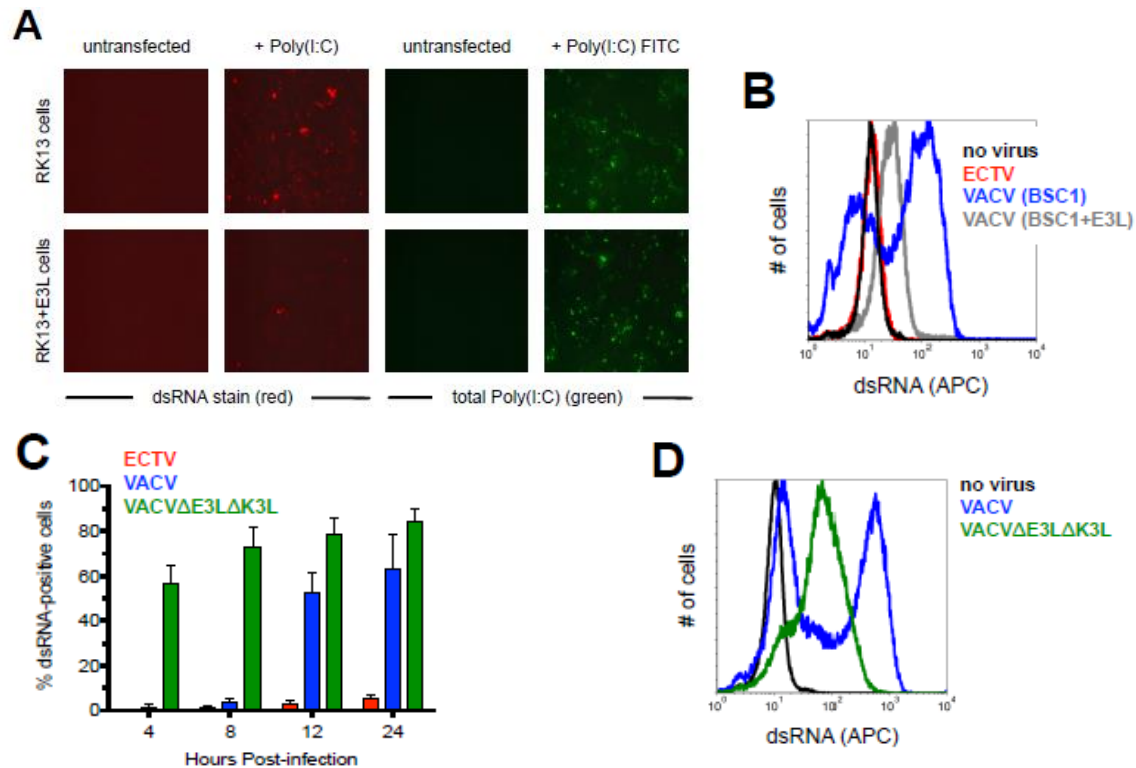
Figure 2: The E3 protein prevents recognition of dsRNA by the J2 antibody. (A) RK13 or RK13+E3L cells were transfected with 1 μg of Poly(I:C) followed by dsRNA staining approximately 16 hrs. later. Methods were repeated using Poly(I:C) conjugated to FITC to determine transfection efficacy. **(B)** BSC1 or BSC1+E3L cells were infected (MOI=10) with either ECTV or VACV for 24 hrs. prior to staining for dsRNA using a secondary antibody conjugated to APC. Flow cytometric data are representative of three independent trials. **(C)** BSC1 cells were infected (MOI=10) with ECTV, wild-type VACV, or VACVΔE3LΔK3L for various lengths of time prior to staining for dsRNA using flow cytometry. Bars depict the average values and error bars represent the standard deviations of three independent trials for each time point. **(D)** BSC1 cells were infected (MOI=10) with VACV or VACVΔE3LΔK3L for 24 hrs. prior to staining for dsRNA using a secondary antibody conjugated to APC. **(E)** BSC1 cells were infected (MOI=10) with VACV, wild-type ECTV, or a mutant of ECTV in which the native E3L gene was replaced with the gene for VACV E3L. After 24 hrs., cells were stained for dsRNA. Flow cytometric data are representative of three independent trials.
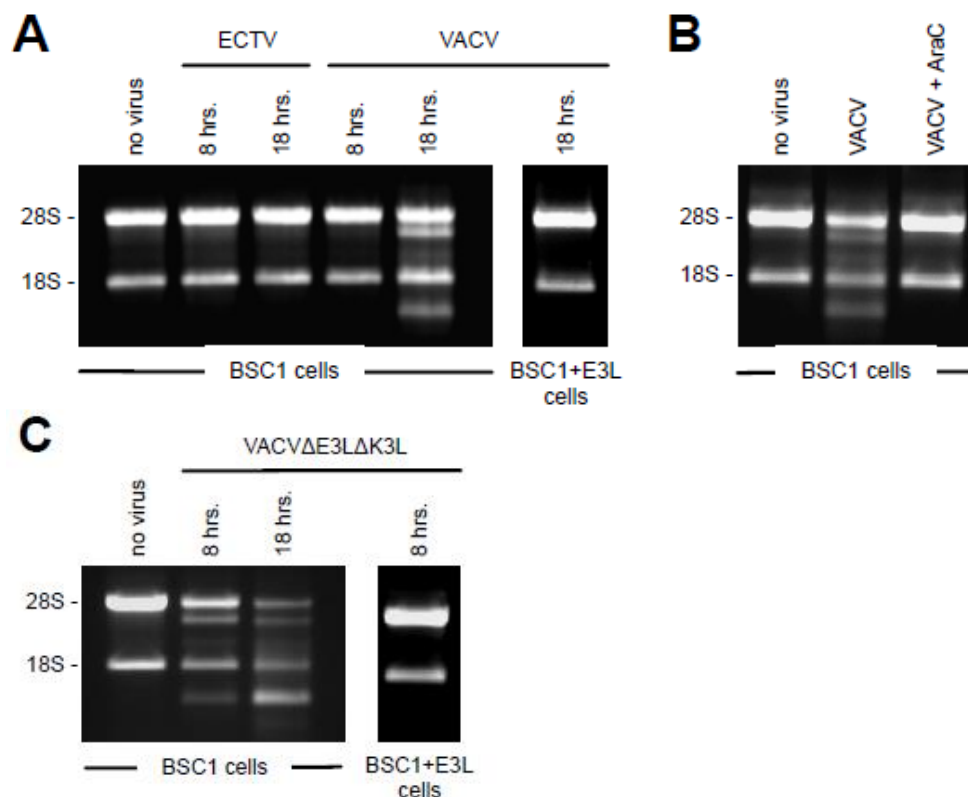
Figure 3. **RNase L activity is not seen in ECTV-infected cells.** **(A)** Total RNA was isolated from BSC1 or BSC1+E3L cells infected with either ECTV or VACV after 8 or 18 hours. Gel electrophoresis was performed on 5 mg of total RNA to monitor for RNA degradation, indicating RNase L activation. **(B)** BSC1 cells were infected with VACV or VACV followed by AraC treatment. RNA was isolated after 18 hours and gel electrophoresis was performed to determine the state of activation of RNase L. **(C)** BSC1 or BSC1+E3L cells were infected with VACVΔE3LΔK3L. RNA was isolated after 8 and 18 hours and gel electrophoresis was performed to determine the state of activation of RNase L.
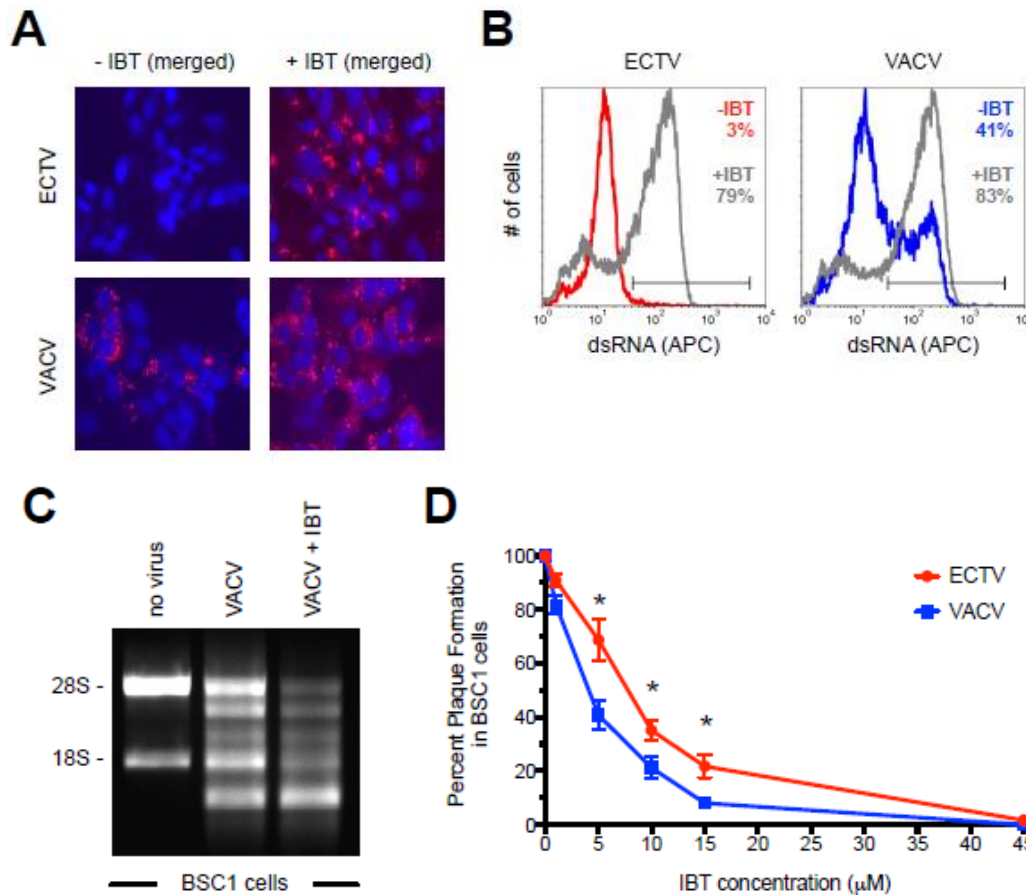
Figure 4: Both ECTV and VACV are sensitive to the anti-poxvirus drug IBT. (A) BSC1 cells were infected (MOI=10) with either ECTV or VACV for 24 hrs. prior to staining for cell nuclei/virus factories and dsRNA. IBT (45 μM) was added at the time of infection. **(B)** BSC1 cells were infected (MOI=10) with either ECTV or VACV for 24 hrs. prior to staining for dsRNA using a secondary antibody conjugated to APC. IBT (45 μM) was added at the time of infection. Percentages represent the fraction of cells that fell within the positive gate. **(C)** RNase L activity assay was performed on cells infected with VACV (MOI=10) or VACV+IBT (MOI=10; 45 μM IBT) 18 hours prior to the isolation of total RNA. Gel electrophoresis was performed on 5 mg of RNA samples. **(D)** Plaque reduction assays were performed on confluent monolayers of BSC1 cells in six-well plates infected with approximately 50 plaque forming units of either ECTV or VACV. IBT was added to the cells at the following concentrations: 0, 1, 5, 10, 15, and 45 μM. Plaques were visualized using crystal violet after two days of incubation for VACV and five days for ECTV. Indicated percentages are relative to the no drug control wells. Graphed values are average values and error bars represent the standard deviation of the mean. Data are an assembly of eight independent plaque reduction assays for each virus.
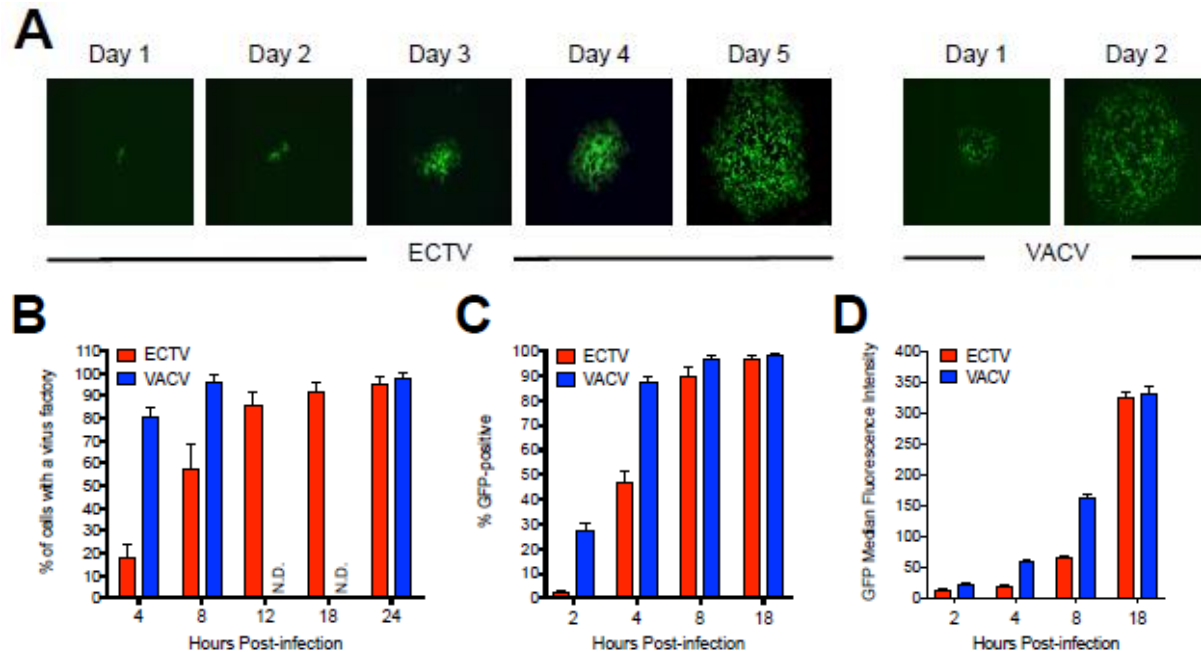
Figure 6: ECTV exhibits delayed replication kinetics relative to VACV. (A) Confluent monolayers of BSC1 cells were initially infected at a low MOI (~0.001) to allow for proper visualization of plaque development over time. ECTV and VACV used were engineered to express GFP. All images are at 50x total magnification. **(B)** BSC1 cells were infected (MOI=10) with either ECTV or VACV for 24 hrs. Virus factories were identified using DAPI staining. For each time point, 150 randomly viewed cells within each infection condition were scored as either positive or negative for the presence of a virus factory of any size. Bars depict the average values and error bars represent standard deviations of two independent experiments. VACV data were not acquired for the 12, 16, and 20 hr. time points because cells were already virtually 100% positive for virus factories by 8 hrs. **(C)** BSC1 cells were infected with ECTV or VACV engineered to express GFP. Flow cytometry was performed at 2, 4, 8, and 18 hrs. post-infection to monitor the amount of cells positive for GFP, indicating viral replication. **(D)** Median fluorescent intensities for each data point in previous figure panel were calculated.
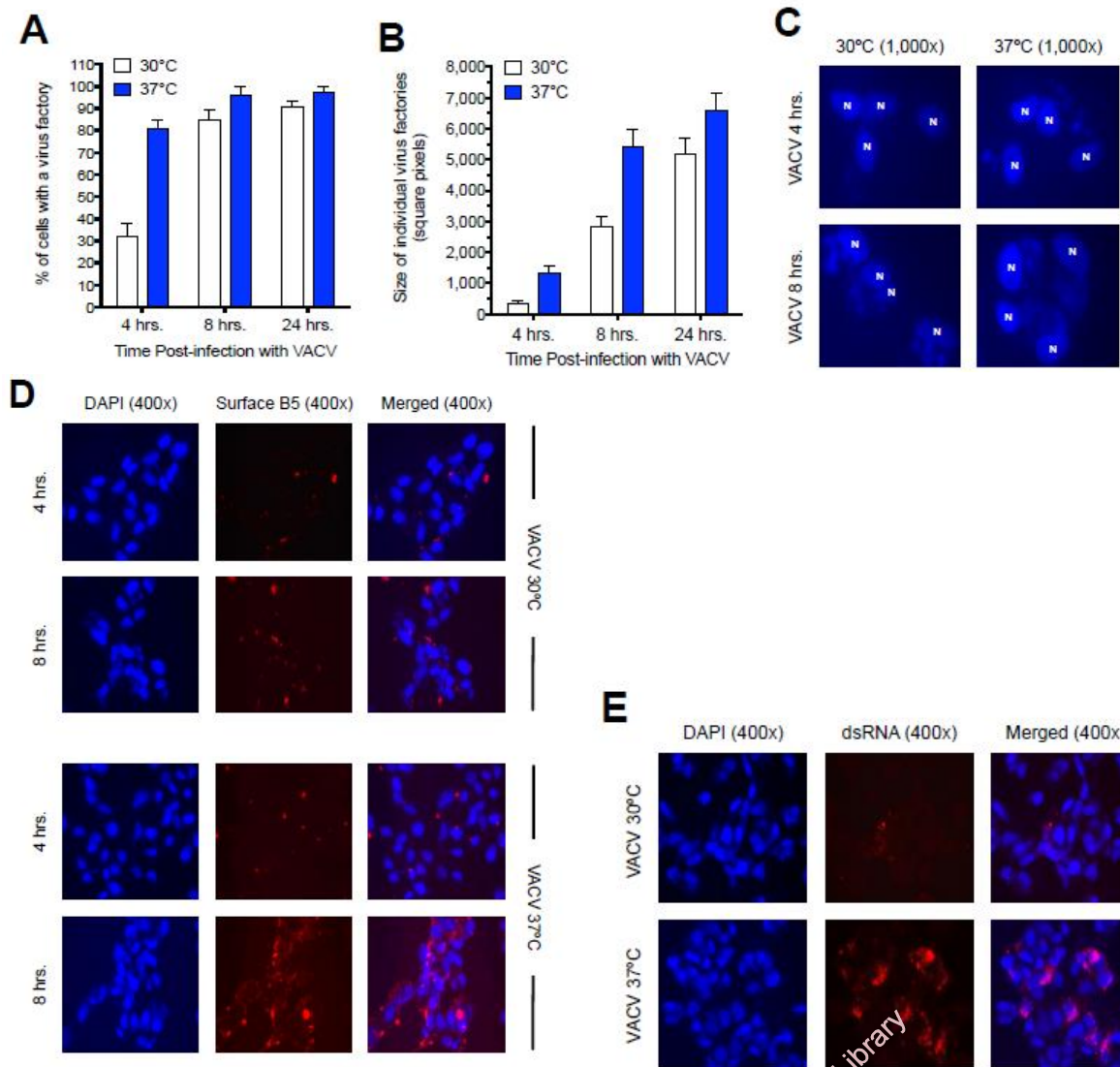
Figure 7: VACV exhibits delayed replication kinetics when grown at 30 °C compared to 37 °C. (A) BSC1 cells were infected (MOI=10) with VACV and then incubated at either 30 °C or 37 °C for 4, 8, or 24 hrs. Virus factories were identified using DAPI staining. For each condition, 150 randomly viewed cells were scored as either positive or negative for the presence of a virus factory of any size. Bars depict average values and error bars represent standard deviations of two independent trials. **(B)** Using the same data from the previous figure panel, images of virus factories were acquired and then analyzed using ImageJ software. The total size of a minimum of 25 virus factories was determined for each condition. Bars depict average values and error bars represent standard deviations. **(C)** Representative images of virus factories are shown for the 4 hr. and 8 hr. time points for both temperatures. Cell nuclei are labeled as "N" in the images, which are at 1,000x total magnification. **(D)** BSC1 cells were infected (MOI=10) with VACV and incubated at either 30 °C or 37 °C for 4 or 8 hrs. Cells were stained for cell nuclei/virus factories and cell surface B5 protein. Images are representative of two independent trials. **(E)** BSC1 cells were infected (MOI=10) with VACV and incubated at either 30 °C or 37 °C for 24 hrs. Cells were stained for cell nuclei/virus factories and dsRNA. Images are representative of three independent trials.

Discussion

Double-stranded RNA formation is seen amongst poxviruses due to their genome layout and mechanisms of transcription. Convergent transcription of tightly packed genes causes the RNA polymerase to read through one gene into the next, resulting in the formation of complementary mRNA that can base pair to form dsRNA. The poxvirus gene, E3L, encodes a protein containing a conserved dsRNA-binding domain (Chang and Jacobs 1993) that acts to shield dsRNA from immune cells, preventing the activation of cellular defenses including PKR and RNase L. In this study, the monoclonal antibody J2 was used, which specifically binds to dsRNA of at least 40 bp in length (Schönborn et al. 1991; Bonin et al. 2000). It was speculated that if E3 can mask dsRNA from recognition by host cell proteins, then it may also prevent binding of J2 to its epitope on dsRNA. The data support this hypothesis as VACV infection of BSC1 cells that constitutively express high levels of E3 displayed significantly reduced dsRNA accumulation relative to the wild-type, E3-negative cells. The dsRNA mimic, Poly(I:C), also lends support to this idea as less of this molecule was detected in RK13+E3L cells than in RK13 plain cells. Based on this, the J2 antibody can only likely detect dsRNA that is not bound by E3, or free dsRNA.

A time course comparing wild-type VACV to VACVΔE3LΔK3L, which lacks E3L, shows that dsRNA is formed in VACV between 8 and 12 hrs. post-infection; however, J2 cannot detect it because it is bound by E3. After 12 hours, levels of dsRNA transitioned from essentially undetectable to greater than half the cells being dsRNA-positive. This supports the notion that E3 shields dsRNA from detection to a point. Nonetheless, after large amounts of dsRNA are produced, E3 is not sufficient to shield the molecule from immune detection. This is likely of little consequence for VACV because K3 is present to act as an additional defense against PKR

when free dsRNA is present. Indeed, wild-type VACV does not readily activate PKR during infection despite the presence of free dsRNA (Langland and Jacobs 2004; Hand et al. 2015).

RNase L activity assays further support this idea. Because dsRNA activates RNase L, shielding of the molecule by E3 would prevent immune detection of dsRNA, preventing RNase L activation. However, at approximately 18 hrs. post-infection, RNase L induction is seen in VACV-infected cells. This indicates that dsRNA formation is above the threshold of E3 binding capacity, causing this immune pathway to activate. In contrast, ECTV does not induce RNase L, supporting the hypothesis that less free dsRNA is produced in ECV-infected cells. Therefore, E3 in ECTV can readily bind to the dsRNA that is formed during replication, preventing the activation of RNase L.

As previously mentioned, the RNA polymerase in VACV does not efficiently terminate at the end of many viral genes, which is most prominently seen during the transcription of intermediate and late genes. This causes the RNA polymerase to read through into the next gene (Broyles 2003), leading to transcripts that are homogeneous near the 5' end but heterogeneous at the 3' end (Xiang et al. 1998; Xiang et al. 2000) which increases the likelihood of dsRNA formation through complementary base pairing. While efficient termination of transcripts would be an effective way to decrease the amount of total dsRNA formed within cells, the IBT susceptibility data suggest that VACV and ECTV do not differ with respect to the extent of transcriptional read-through. Monkeypox virus (MPXV) accumulates less free dsRNA and, unlike ECTV and VACV, is naturally resistant to IBT and forms shorter transcripts (Arndt et al. 2016). Notably, it has been shown that IBT-resistant mutants of VACV form shorter transcripts late during infection in the absence of the drug (Cresawn et al. 2007). Therefore, even though both ECTV and MPXV form less free dsRNA, the underlying mechanisms used to achieve this

seem quite distinct. To further reinforce this point, Arndt et al. (2016) observed an increase in dsRNA staining using the J2 antibody in VACV-infected – but not MPXV-infected – cells treated with IBT relative to the no drug control. While this study indicated similar results for VACV-infected cells as these authors, there was a striking increase in dsRNA staining within ECTV-infected cells treated with IBT compared to untreated cells.

These data suggest that ECTV relies on a protracted replication cycle to generate less free dsRNA relative to VACV. Support for this was seen through VACV infections performed at 30 °C compared to 37 °C, which resulted in significantly lower levels of dsRNA in cells incubated at the lower temperature. Double-stranded RNA staining in VACV-infected cells grown at 30 °C looked nearly identical to dsRNA staining in wild-type ECTV, indicating that the lower temperature could artificially delay VACV replication. Therefore, it is speculated that by slowing its replication cycle, ECTV is better able to manage the effects of generating dsRNA. The protracted replication kinetics seen in ECTV result in less mRNA formed per unit of time, decreasing the opportunity for the formation of dsRNA relative to VACV.

This study shows that ECTV forms less detectable dsRNA than VACV after infection in multiple cell lines. This is speculated to be a compensatory mechanism because ECTV does not produce a functional K3 protein due to a premature stop codon within the open reading frame of the K3L gene (Chen et al. 2003; Smith and Alcami 2002). Therefore, by lacking K3, ECTV seemingly relies on E3 as its main defense against PKR activation. This is similar to what is seen in MPXV, which also lacks K3L and produces less dsRNA relative to VACV (Arndt et al. 2016), lending further support to this idea. Conversely, many other orthopoxviruses, such as VACV and CPXV, produce both E3 and K3 giving them two defense systems against the activation of innate immune pathways. This was seen through the experiments with CPXV, which also contains a

functional K3L gene and produces dsRNA levels like that of VACV. Thus, ECTV seems to act by accumulating lower levels of dsRNA, decreasing the possibility of activating innate immune pathways within cells, which likely made the loss of K3 less detrimental to the virus during its evolutionary history.

Future research for this study will include the analysis of transcript heterogeneity between ECTV and VACV to determine if the two differ in transcription termination. Northern blotting will be performed between ECTV and VACV-infected cells to determine if ECTV is more efficient at transcription termination, thereby resulting in the formation of less dsRNA because of less transcriptional read-through. It is hypothesized that kinetics is the main mechanism used by ECTV to form less dsRNA; therefore, performing this assay can help to determine if slower replication is the main mechanism utilized by this virus or if transcription termination may play a role as well. Further, real-time polymerase chain reaction (PCR) will be performed to analyze the level of gene expression of a known late gene over time between ECTV and VACV-infected cells. It is predicted that ECTV will show a delay in gene expression relative to VACV. These data can then help to determine how ECTV and VACV compare in their gene expression, which can be indicative of their overall kinetics differences. Overall, these assays will play a vital role in the finalization of this project.

Acknowledgements

Literature Cited

Aranda PS, LaJoie DM, Jorcyk CL. (2012) Bleach gel: A simple agarose gel for analyzing RNA quality. *Electrophoresis, 33,* 366–369.

Arndt WD, White SD, Johnson BP, Huynh T, Liao J, Harrington H, Jacobs BL. (2016) Monkeypox virus induces the synthesis of less dsRNA than vaccinia virus, and is more resistant to the anti-poxvirus drug, IBT, than vaccinia virus. *Virology*, *497*, 125-135.

Bayliss CD, Condit RC. (1993) Temperature-sensitive mutants in the vaccinia virus A18R gene increase double-stranded RNA synthesis as a result of aberrant viral transcription. *Virology, 194,* 254–262.

Beattie E, Kauffman EB, Martinez H, Perkus ME, Jacobs BL, Paoletti E, Tartaglia J. (1996) Host-range restriction of vaccinia virus E3L-specific deletion mutants. *Virus Genes 12,* 89–94.

Bonin M, Obersrab J, Lukas N, Ewert K, Oesterschulze E, Kassing R, Nellen W. (2000) Determination of preferential binding sites for anti-dsRNA antibodies on double-stranded RNA by scanning force microscopy. *RNA, 6,* 563-570.

Brennan G, Kitzman JO, Rothenburg S, Shendure J, Geballe AP. (2014) Adaptive gene amplification as an intermediate step in the expansion of virus host range. *PLoS Pathogens, 10,* e1004002.

Broyles SS. (2003) Vaccinia virus transcription. *J Gen Virol., 84,* 2293–2303.

Chang HW, Jacobs BL. (1993) Identification of a conserved motif that is necessary for binding of the vaccinia virus E3L gene products to double-stranded RNA. *Virology, 194*, 537–547.

Chang HW, Watson JC, Jacobs BL. (1992) The E3L gene of vaccinia virus encodes an inhibitor of the interferoninduced, double-stranded RNA-dependent protein kinase. *Proc. Natl. Acad. Sci. USA, 89*, 4825-4829.

Chen N, Danila MI, Feng Z, Buller ML, Wang C, Han X, Lefkowitz EJ, Upton C. (2003) The

genomic sequence of ectromelia virus, the causative agent of mousepox. *Virology, 317,* 165–186.

Cresawn SG, Prins C, Latner DR, Condit RC. (2007) Mapping and phenotypic analysis of spontaneous isatin-β-thiosemicarbazone resistant mutants of vaccinia virus. *Virology, 363,* 319-332.

Díaz-Guerra M, Rivas C, Esteban M. (1997) Inducible xxpression of the 2-5A synthetase/RNase L system results in inhibition of vaccinia virus replication. *Virology, 227,* 220-228.

Earl PL, Moss B. (2001) Characterization of recombinant vaccinia viruses and their Products. *Current Protocols in Protein Science*, 13:5.14:5.14.1–5.14.11.

Fang M, Lanier LL, Sigal LJ. (2008) A role for NKG2D in NK cell-mediated resistance to poxvirus disease. *PLoS Pathogens, 4,* e30.

Fenner F. (1947) Studies in infectious ectromelia in mice (mouse pox) natural transmission; elimination of the virus. *Aust J Exp Biol Med Sci., 25,* 327-335.

Hand ES, Haller SL, Peng C, Rothenburg S, Hersperger AR. (2015) Ectopic expression of vaccinia virus E3 and K3 cannot rescue ectromelia virus replication in rabbit RK13 cells. *PloS one*, *10*(3), e0119189.

Jacobs BL, Langland JO. (1996) When two strands are better than one: the mediators and modulators of the cellular responses to double-stranded RNA. *Virology, 219,* 339–349.

Langland JO, Jacobs BL. (2004) Inhibition of PKR by vaccinia virus: role of the N- and C-terminal domains of E3L. *Virology, 324*, 419-429.

Prins C, Cresawn SG, Condit RC. (2004) An isatin-beta-thiosemicarbazone-resistant vaccinia virus containing a mutation in the second largest subunit of the viral RNA polymerase is defective in transcription elongation. *J. Biol. Chem., 279*, 44858–44871.

Rahman MM, Liu J, Chan WM, Rothenburg S, McFadden G. (2013) Myxoma virus protein M029 is a dual function immunomodulator that inhibits PKR and also conscripts RHA/DHX9 to promote expanded host tropism and viral replication. *PLoS Pathogens, 9,* e1003465.

Schönborn J, Oberstrass J, Breyel E, Tittgen J, Schumacher J, Lukacs N. (1991) Monoclonal antibodies to double-stranded RNA as probes of RNA structure in crude nucleic acid extracts. *Nucleic Acids Research, 19,* 2993–3000.

Smith VP, Alcami A. (2002) Inhibition of interferons by ectromelia virus. *Journal of Virology, 76,* 1124–1134.

Watson JC, Chang HW, Jacobs BL. (1991) Characterization of a vaccinia virus encoded double-stranded RNA binding protein that may be involved in the inhibition of the double stranded RNA dependent protein kinase. *Virology, 185,* 206-216

Weber F, Wagner V, Rasmussen SB, Hartmann R, Paludan SR. (2006) Double-stranded RNA is produced by positive-strand RNA viruses and DNA viruses but not in detectable amounts by negative-strand RNA viruses. *J. Virol. 80,* 5059-5064.

Xiang Y, Latner DR, Niles EG, Condit RC. (2000) Transcription elongation activity of the

vaccinia virus J3 protein in vivo is independent of poly(A) polymerase stimulation. *Virology, 269,* 356–369.

Xiang Y, Simpson DA, Spiegel J, Zhou A, Silverman RH, Condit RC. (1998) The vaccinia virus A18R DNA helicase is a postreplicative negative transcription elongation factor. *J. Virol., 72,* 7012–7023.